Feature article

Metabolic Network Modelling of Chinese Hamster Ovary (CHO) Culture Bioreactors Operated as Microbial Cell Factories

Jernej Gašperšič,[1,2,*] Miha Kastelic,[2] Uroš Novak[2] and Blaž Likozar[2]

[1] *Institute of Biochemistry, Medical faculty, University of Ljubljana, Vrazov trg 2, 1000 Ljubljana*

[2] *National Institute of Chemistry, Department of Catalysis and Chemical Reaction Engineering, Hajdrihova 19, 1000 Ljubljana, Slovenia*

* *Corresponding author: E-mail: jernej.gaspersic@mf.uni-lj.si*

Received: 06-07-2018

Abstract

Chinese hamster ovary (CHO) epithelial cells are one of the most used therapeutic medical lines for the production of different biopharmaceutical drugs. They have a high consumption rate with a fast duplication cycle that makes them an ideal biological clone. The higher accumulated amounts of toxic intracellular intermediates may lead to lower organism viability, protein productivity and manufactured biosimilar, so a careful optimal balance of medium, bioreactor operational parameters and bioprocess is needed. A precise phenomenological knowledge of metabolism's chemical transformations can predict problems that may arise during batch, semi-continuous fed batch and continuous reactor operation. For a better detailed understanding (and relations), future performance optimization and scaling, mechanistic model systems have been built. In this specific work, the main metabolic pathways in mammalian structured CHO cultures are reviewed. It starts with organic biochemical background, controlling associated phenomena and kinetics, which govern the sustaining conversion routes of biology. Then, individual turnover paths are described, overviewing standard mathematical formulations that are commonly applied in engineering. These are the core of black box modeling, which relates the substrates/products in a simplified relationship manner. Moreover, metabolic flux analysis (MFA)/flux balance analysis (FBA), that are traditionally characterizing mechanisms, are presented to a larger portion extent. Finally, similarities are discussed, illustrating the approaches for their structural design. Stated variables' equations, employed for the description of the growth in the controllable environmental conditions of a vessel, the researched reaction series of proliferating dividing CHO population, joint with the values of maximal enzymatic activity, and solutions are outlined. Processes are listed in a way so that a reader can integrate the state-of-the-art. Our particular contribution is also denoted.

Keywords: Microbial cell factory; Chinese hamster ovary (CHO) cell metabolism; Bioreactor operation modeling; Biochemical reaction kinetics; Metabolic flux analysis; Biopharmaceutical and biosimilar

1. Introduction

Chinese hamster ovary (CHO) cells are one of the most important cell lines for production of therapeutic biopharmaceuticals.[1,2] CHO cells are characterized by high consumption rates of nutrients and large amount of toxic intermediates, which may lead to lower cell viability and protein production.[1,2,3] Production of recombinant proteins is promoted in growth medium with high content of glucose and glutamine.[4,5] Further optimization of the medium is needed to reduce lactate and ammonia accumulation and to increase antibody yields.[3,6–9] In recent years technology has made a remarkable impact in bioreactor fermentation yields using kinetic models that are commonly used to describe fermentation processes in industrial fermentors. These models turn out to be useful at process monitoring, acquiring and storing the data, and troubleshooting. In the last three decades databases of CHO cell metabolism have been extended, likewise the tracing of fluxes into biomass and byproducts, which led to major improvements of bioreactor models.[2,5,10–17] This knowledge has guided the researchers to develop several mathematical models, which are able to describe the fluxes within metabolic pathways.[4,18–23]

Analysis of fluxes usually focuses on measuring concentrations of extracellular metabolites.[13] Biocatalysis of substrates into commercially attractive products as well as byproducts is connected through pathways of cell metabolism.[13,24–26] Pathway analysis usually relies on measuring concentration behavior of extracellular metabolites,[13] nev-

ertheless estimates of intracellular fluxes are readily available by using flux balance analysis (FBA) and metabolic flux analysis (MFA).[27] In recent years genotype data have been also included into *in silico* methodologies.[28] The following pathways of the cell metabolism are usually assumed: glycolysis, pentose phosphate (PPP) pathway, tricarboxylic acid (TCA) cycle, amino acid metabolism, protein synthesis, urea cycle, nucleic acid synthesis, membrane lipid synthesis, and biomass production.[1–5,14–19,29–36] Glycogen[5,16] synthesis and glycosylation pathways are part of detailed models.[29,37–41]

Numerous models were developed for the purpose of data analysis and growth optimization in cell cultures. A hybrid simulation framework was proposed to predict the dynamics in bioreactors.[42] A simplified model of central carbon metabolism provides the framework for analyzing measurements of external metabolites.[29] Simulation assuming pseudo steady state assumption and extracellular metabolite concentrations accurately predicted the effects of process variables, temperature shift, seeding density, specific productivity and nutrient concentrations.[43] A mathematical model was developed for optimization of batch and fed batch bioreactor.[20] The kinetic model that jointed several phases of cell culture was capable to describe the time evolution of experimental data.[16] Similar model was build and its correctness validated on experimental data from CHO cells grown in spinner flasks.[19] The model was assembled from submodels, where each of them described a separate phase of CHO cell (growth, stationary, and decline phase).[33] The model was then used to explain the experimental data from batch cultivated CHO cells. In another example, the phenotype of mammalian cells was studied by the aims of metabolic flux analysis.[5] Fluxes were measured using ^{13}C MFA variant and stoichi-

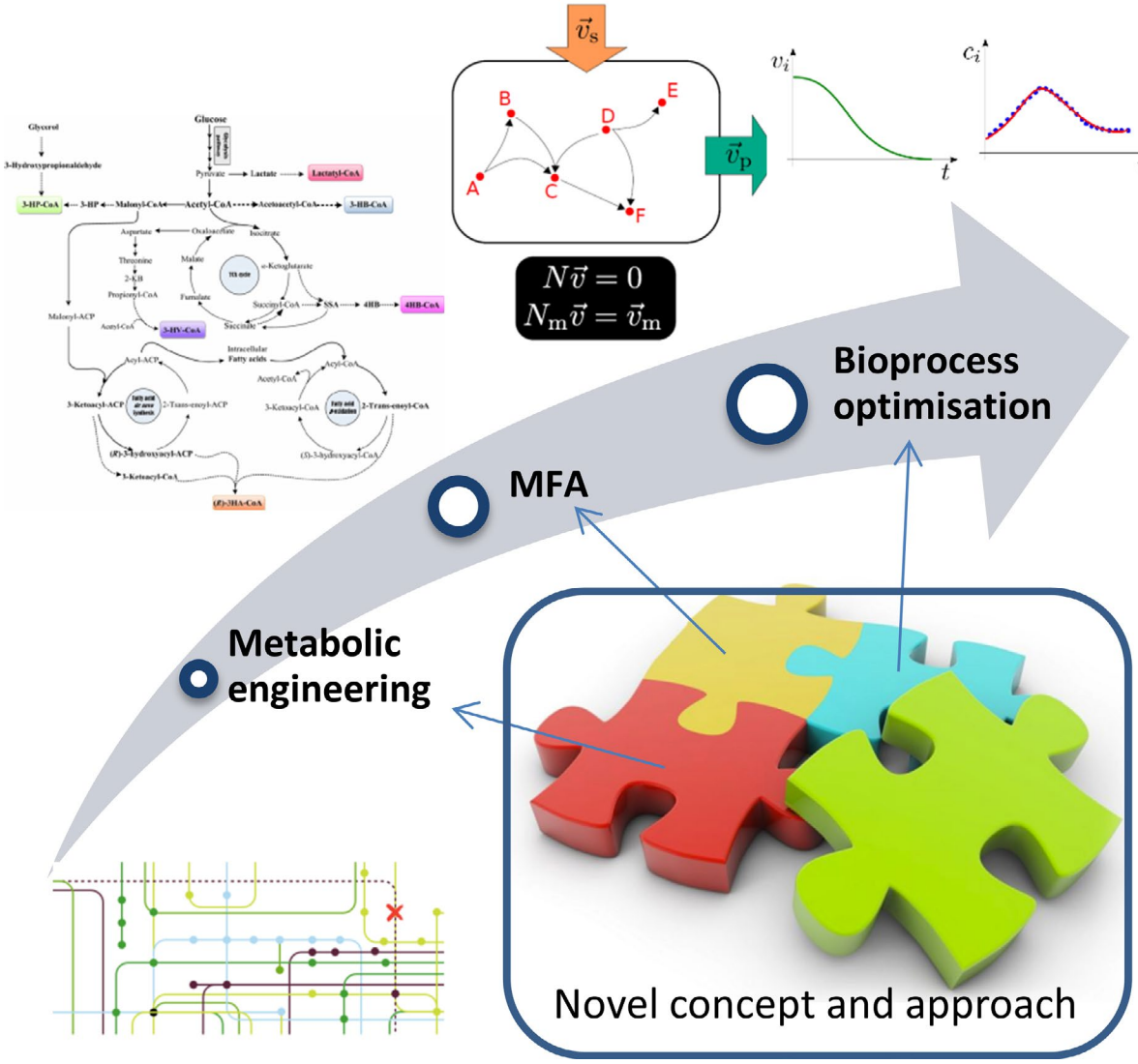

Figure 1: Metabolic engineering starts with the metabolic network, which comprises biochemical transformations within living cells (bottom left: unstructured network, top left: structured network). Then we use available experimental data together with theoretical methodologies (paradigm of Metabolic Flux Analysis – MFA) to estimate flux rates of biochemical transformations (top right). These insights help us to perform bioprocess optimization.

ometric modeling.[2,44] MFA was also used to estimate total energy production of growing CHO-320 cells.[24]

New metabolic information was mined from the models and associated simulations. Analysis of experiments showed the existence of multiple steady states.[17] *In silico* modeling of CHO cells allowed the identification of major growth-limiting factors including oxidative stress and depletion of lipid metabolites.[45] These factors may lead to a better development of strategies to enhance CHO culture performance.[45] Continuous cell lines can down-regulate their oxidative metabolism when nutrients get depleted or growth rate slows.[15] Flux analysis shows significant rewiring of intracellular metabolic fluxes in the transition from growth to stationary phase. Changes were noticed in energy metabolism, redox metabolism, oxidative pentose phosphate pathway and anaplerosis.[16] In stationary phase glycolysis is rerouted through PPP pathway – no lactate production is observed.[2] Unusual lipogenic pathway was discovered with modeling. Carbon from glucose supplies mitochondrial production of alpha-ketoglutarate (αKG), which is trafficked to the cytosol and used to supply reductive carboxylation by isocitrate dehydrogenase.[46] It was suggested that endogenous lactate is not being used for ATP production through TCA cycle when the medium is supplemented with galactose. It was observed that lactate starts to get depleted at the same time as glucose is used up and cell switches to a galactose source.[1] With kinetic model of CHO cell growth Lopez-Meza estimated substrate threshold below which growth is not observed and obtained the α and β factor from Luedeking-Piret equation.[18] Analysis showed that CTP deficient cells use different central carbon metabolism, suppress pyruvate dehydrogenase, and induce glucose dependent anaplerosis through pyruvate carboxylase.[46]

Composition optimization of limiting amino acids in growth medium increased maximum cell density by 55% and protein titer production by 27%.[3] The medium did not have any influence on sialic acid content. Mannose carbon source also improved recombinant protein productivity.[47] Glucose consumption was 5 times higher than that of glutamine (^{13}C labeled glucose, 2D-NMR spectroscopy). Error propagation of Goudar metabolic flux analysis can be routinely used in bioprocess development.[14] Modeled effect of specific rate error on the flux error is a function of both the sensitivity of the flux with respect to the specific rate and relative magnitudes of the flux and the specific rate.[14] 41% of glucose was channeled through PPP, while flux of pyruvate to lactate and to TCA cycle was evenly distributed 55%–45%; anaplerotic conversion to oxaloacetate accounted to 10% of whole pyruvate conversion.[14]

We describe the research done in the area of bioreactor modeling and contribution of our department to the field. Complete literature search and data collection of known metabolic fluxes was made to ease the design of future models. The improvement of models is ongoing with a goal to make a good theoretical framework and to foresee possible errors in the fermentation process. Schematic illustration of the interplay between metabolic engineering and bioprocess is shown in Figure 1.

2. Contribution of the Authors

Modeling brings new insights into existing problems. Great advantage of modeling is to track the problem at molecular, cellular level. Good hypothesis and theories cannot be developed without sufficiently developed model. Development of biotechnology processes is thus easier and cost effective. Models have many disadvantages, because they may be developed on unproven hypothesis or theories that yet need to be confirmed. Theories may have in this case erroneous core.

Complete literature search of published models and metabolism of CHO cells leads to a successful build of model of bioreactor. Review of preferred articles is included with the emphasis on bioreactor operation equations and metabolic pathways of CHO cell lines.

Contribution is divided into three parts:

- Overview of black box models: Evolution of mathematical equations used in CHO mechanistic models
- Overview of CHO cell metabolic pathways and the unique properties of CHO cell lines
- Overview of mechanistic models and our proposed approach toward solution of the problem

2. 1. Review of Black Box Models: Formulation of Mathematical Equations

Protein production in a bioreactor requires perfect agitation and aeration to maintain a homogeneous distribution of cells, substrate and oxygen throughout the bioreactor. Extracellular medium composition analysis, coupled with intracellular metabolic pathway analysis give rise to CHO cell bioreactor models.

2. 1. 1. Growth of Biomass

Growth of biomass is described in different ways. Growth is influenced by the specific growth factor (μ) and concentration of cells (X) as seen in Eq. (1).[16,19,20]

Standard biomass growth equation:

$$\frac{\mathrm{d}X}{\mathrm{d}t} = \mu X \tag{1}$$

Specific growth factor (μ) is described in different ways. Commonly used descriptions are Verhulst and Monod equations, which can be adequately modified to account for bioreactor conditions (Eqs. 2 and 6).

One limit substrate Monod[36] kinetics is:

$$\mu = \mu_{\max} \frac{[S]}{[S] + K_S} \tag{2}$$

while two limit substrates Monod[24] kinetics is expressed as:

$$\mu = \mu_{max} \frac{[S_1]}{[S_1]+K_{S_1}} \frac{[S_2]}{[S_2]+K_{S_2}} \quad (3)$$

and finally *n*-limit substrates Monod[24] kinetics as:

$$= \mu_{max} \frac{[S_1]}{[S_1]+K_{S_1}} \frac{[S_2]}{[S_2]+K_{S_2}} \times \ldots \times \frac{[S_n]}{[S_n]+K_{S_n}} \quad (4)$$

By Monod, biomass growth is influenced by limiting substrate (Eq. 2). Here X represents cell concentration – number of cells per mL; S represent substrate, μ_{max} is the maximum value of growth rate, K_S is the substrate saturation constant. Note that specific growth rate (μ) may be influenced by one limiting substrate (Eq. 2),[18] two (Eq. 3)[37] or more limiting substrates from the growth medium (Eq. 4).[48]

del Val[38] proposed modified expression:

$$\mu = \mu_g \left[\frac{[S]}{K_m+[S]} - \frac{[X_v]}{\alpha_x}\right] \quad (5)$$

By del Val, an upgraded Monod equation for continuous production is utilized, where X_v is the density of viable cells and α_x is the specific factor (cellular carrying capacity). Viable cells represent live cell population, while total cells represent a sum of viable and dead cell population. The ratio is changing through cell phases. Each equation is optimized for specific value, so it is necessary to take into account certain value.

Verhulst[49] established the following closure:

$$\mu = \mu_{max} \left(1 - \frac{X}{X_{max}}\right) \quad (6)$$

By Verhulst, maximum cell density of the culture (X_{max}) is a limiting factor to cell growth. In this case substrate is available in large quantities or may be fed additionally to the bioreactor. The equation is commonly used to describe the growth of bacterial cultures.

Equations for biomass growth that are commonly used in bioreactor systems are described below (continuous, fed batch).

Altamirano[17] and Xing[3] suggested to use the following formulation:

$$\mu = D \frac{X_T}{X_V} \quad (7)$$

By Altamirano, the specific growth rate in the continuous bioreactor is described as dilution rate (D) multiplied by the ratio of the total cell number (X_T) and the viable cell number (X_V).

Goudar[4] wrote the growth factor (μ) as:

$$\mu = \frac{F_d}{V} + \frac{F_h}{V}\frac{X_V^H}{X_V^B} + \frac{1}{X_V^B}\frac{dX_V^B}{dt} \quad (8)$$

By Goudar, the specific growth rate is designed for perfusion systems, where V is the reactor volume, F_d is the discard rate, F_h is the harvest flow rate, X_V^H is the harvest viable cell density, and X_V^B is the density of viable cells in bioreactor.

Hagrot[21] used the solution of first-order kinetics:

$$\mu = \frac{ln\left(\frac{X_v}{X_{v,0}}\right)}{t-t_0} \quad (9)$$

By Hagrot, the specific growth rate depends upon viable cell concentration before renewal (X_v) and after renewal (X_{v0}). Here t and t_0 are corresponding times of sampling.

It is essential for the model of bioreactor to select the mathematical formulation that suits type of the bioreactor and the cell culture. To get the best formulation we need to compare numerical simulations with experimental data and choose the best fitting curve. For that we need a set of sensor concentration data of products, substrates, and biomass in bioreactor throughout fermentation process.

2. 1. 2. Final Product Formation

Final product formation is described in connection with the cell concentration (X) or viable cell concentration (X_v) multiplied by product growth factors (r or α) (Eq. 10 and 11).[20,33]

Standard equation to describe product formation:

$$\frac{dP}{dt} = rX \quad (10)$$

Naderi[20] and Provost[19] wrote down the following closure:

$$\frac{dP}{dt} = \alpha_g X_v \quad (11)$$

while Ludeking-Piret[35] suggested additional term:

$$\frac{dP}{dt} = \alpha \frac{dX}{dt} + \beta X \quad (12)$$

By Ludeking-Piret, two coefficients α and β describe the product formation, both are product specific. Further, P is the concentration of glycosylated product, and dX/dt is the slope of biomass increase.

Xing[3] and Berrios[47] suggested two formulations:

$$\frac{dP}{dt} = \frac{D\left(C_i^{out} - C_i^{in}\right)}{X_V} X \quad (13)$$

$$\frac{dP}{dt} = \frac{C_i(t_2) - C_i(t_1)}{IVCD_i(t_2) - IVCD_i(t_1)} X \quad (14)$$

By Xing, product growth is described by the ratio of concentration difference of product (C_i) between two time points. X_v is the viable cell density, and D is the dilution factor (Eq. 13). By Berrios concentration difference of the product (c_i) was divided by the corresponding difference of integral viable cell density (IVCD) (Eq. 14).

Zamorano[24] proposed linear relationship:

$$\frac{dP}{dt} = N_p v(t) X \tag{15}$$

By Zamorano, the *r* factor (Eq. 10) was substituted by multiplication of stoichiometric matrix for final product (N_p) and metabolic flux ($v(t)$).

Goudar[4] utilized the extended closure:

$$\frac{dP}{dt} = \frac{1}{X_V^B}\left(\frac{F_m P}{V} + \frac{dP}{dt}\right) X \tag{16}$$

By Goudar, the product growth consists of two terms. Here X_V^B is viable cell density, and F_m is the flow rate. The equation is used to describe perfusion systems.

del Val[38] used the following expression:

$$\frac{dP}{dt} = \left(Y_{P/S}\right) q_S X \tag{17}$$

By del Val, the expression describes product growth as a yield of product per substrate (Y_{PIS}) multiplied by the substrate consumption (q_S).

The formula for product growth must be developed for each individual product and is based on the observable physical and biochemical strain characteristics and the type of bioreactor. Reviewed models are optimized to describe formation of secondary metabolites – end products.[1–5,15,17,19,21, 24,29,30,31,37,38,40,43,45,46,50] For production of antibodies post translational glycosilation should be taken into account as well.[37,38,40] Formation of primary metabolites – important for growth and maintenance of cell were most precisely described in Quek's model with thorough description of nucleotide and lipid synthesis.[5]

2. 1. 3. Mathematical Description of Substrate Consumption

Substrate consumption is dependent upon cell density (X) and specific uptake rate (v_S) as follows:[17,24,33]

$$\frac{dS}{dt} = -v_S(t)\, X(t) \tag{18}$$

Jedrzejewski[37] proposed the formulation with two terms:

$$\frac{dS}{dt} = \left(\frac{\mu}{Y_{glc}} + m_{glc}\right) X \tag{19}$$

By Jedrzejewski substrate consumption is influenced by number of cells, steady state consumption of substrate (m_{glc}), and biomass growth coefficient (Y_{glc}).

Goudar[4] and Xu[6] suggested another equation:

$$\frac{dS}{dt} = \frac{1}{X_V^B}\left(\frac{F_m(S_m - S)}{V} - \frac{dS}{dt}\right) X \tag{20}$$

By Goudar and Xu specific substrate consumption rate depends upon perfusion rate F_m, difference of substrate concentration (starting minus current) (S_m–S), bioreactor volume (V), and viable cell density (X_V^B).

del Val[38] extended the Michaelis-Menten kinetics as:

$$\frac{dS}{dt} = \left(\frac{1}{Y_{X/S}}\right)\left(\frac{S}{K_m + S}\right) X \tag{21}$$

By del Val, $Y_{X/S}$ is the yield coefficient from substrate, S represents concentration of substrate, K_m is constant specific for each substrate.

Ahn[16] introduced another expression:

$$\frac{dS}{dt} = -k\, S - q_S\, X \tag{22}$$

By Ahn, decomposition of substrate k is independent of biomass. S represents substrate concentration, X represents cell concentration, and q_s is a substrate consumption per cell concentration unit.

2. 1. 4. Oxygen Consumption

Oxygen consumption is traditionally described as follows:[5,17,50]

$$\frac{dDO}{dt} = \mathrm{OTR} - \mathrm{OCR} \tag{23}$$

$$\mathrm{OTR} = K_L a\ (\mathrm{DO^*\text{-}DO}) \tag{24}$$

Oxygen concentration is dependent upon oxygen transfer rate (OTR) between gas and liquid phase and oxygen consumption rate (OCR) of biomass.[29,51] OTR is dependent upon $K_L a$ (bioreactor specific) and dissolved oxygen concentration (DO). Note that saturated oxygen (DO^*) is temperature dependent.[29]

Jorjani[52] used the following expression:

$$OCR = q_{O2}\, X_v;\ q_{O2} = q_{O2}^0\, e^{-E/RT} \tag{25}$$

By Jorjani, OCR is dependent upon q_{O2}^0 and temperature,[52] while q_{O2}^0 is cell culture and clone specific. It depends mostly on the number and condition of mitochondria (origin of respiratory chain). It is also dependent upon availability of substrate with which cell and later mitochondria are fed.[53]

Nyberg[29] proposed two terms:

$$\mathrm{OUR} = K_L a\ (C^*\text{-}C_R) + D\ (C_F\text{-}C_R) \tag{26}$$

By Nyberg, the formula accounts for the continuous bioreactor, where oxygen uptake rate (OUR) is dependent upon OTR as ($K_L a\ (C^* - C_R)$), dilution rate (D), and the difference between oxygen concentrations (feed minus reactor) as ($C_F - C_R$). C^* represents saturated oxygen concentration at operating temperature.

Oxygen is consumed in the respiratory chain. H_2O is the byproduct of the respiratory chain reactions.[54] Oxygen that is incorporated in waste CO_2 comes from glucose or

other substrates. Since metabolism is affected by *p*H value, O_2 consumption (metabolism) is *p*H dependent.[55]

2. 1. 5. CO_2 and NH_3 Waste Production

CO_2 production is integrated into models to address reactions in TCA cycle.[5,45,50] CO_2 is mostly produced in Krebs cycle, while NH_3 is produced during metabolism of glutamine and other amino acids.[5,17,33,56]

$$\frac{\mathrm{dDCO_2}}{\mathrm{d}t} = \mathrm{CO_2PR} - \mathrm{CO_2TR} = \mathrm{K_La\ (DCO2 - DCO2*) + R_{CO2}X} \quad (27)$$

CO_2 concentration is dependent upon CO_2 transfer rate (CO_2TR), and CO_2 production from biomass (CO_2PR). CO_2 importantly influences cell growth and productivity.[57] Free CO_2 can be recycled together with amino group during fixation into carbamoyl phosphate and later integrated into arginine (urea cycle). Dissolved CO_2 (DCO_2) partially transforms into HCO_3^- ions, which serve as a regulator of *p*H in the cell. CO_2 is generated during pyruvate, isocitrate and oxoglutarate degradation (TCA cycle). It is also generated in lysis of lysine and glycine as well as in formation of ribose-6-phosphate from glucose-6-phosphate. R_{CO2} represents rate of CO_2 production.

Nyberg[29] suggested another expression:

$$CER = \frac{n_g}{V_R}(y^R_{CO2} - y^F_{CO2}) + \mathrm{D}\ (C^R_A - C^F_A) \quad (28)$$

By Nyberg, expression accounts for carbon dioxide evolution rate. Here n_g is molar gas flow rate to the reactor, V_R is liquid volume of the reactor, V_R is mole fraction of CO_2 in reactor headspace, y^R_{CO2} is mole fraction of CO_2 in the feed gas. C^R_A is concentration of CO_2 and bicarbonate in the liquid phase, C^F_A is concentration of CO_2 and bicarbonate in the liquid feed phase.

$$\frac{\mathrm{dDNH_3}}{\mathrm{dt}} = \mathrm{NH_3PR} - \mathrm{NH_3TR} = \mathrm{K_La(DNH_3\text{-}DNH_3*) + R_{NH3}X} \quad (29)$$

In Eq. (29), concentration of NH_3 has similar mathematical dependence as CO_2 in Eq. (27). Note that K_La is different for each gas and varies with the reactor and temperature. Ammonia production is highly dependent upon lysis of amino acids that can be biomass dependent and/or independent (catalytic degradation in water medium dependent upon temperature). Ammonia is produced from the amino acids and transferred into gas phase. Then, it is recycled during formation of carbamoyl phosphate.

2. 1. 6. Temperature, *p*H Optimum

Temperature and *p*H are important process parameters that influence optimal growth of CHO cell lines.[58–64] Normal operating temperature for the growth of mammalian cells is 37 °C.[65] At 33 °C a remarkable decrease in specific growth rate is observed. At 30 °C, growth of cells starts to stagnate. Mammalian cells grow in the range from 35 to 38 °C.[55,66] On the other hand, production rate of product (unspecified recombinant protein) is increased at 33 and 30 °C. Lower temperatures (below 37 °C) inhibit cell growth, but enhance cellular productivity of the recombinant protein, maintain high cell viability, suppress consumption of nutrients from medium, and suppress release of waste products from the cells.[67,68]

CHO cells have been reported to grow best at *p*H 7.1.[55] Maximum product concentration (recombinant protein) was achieved at *p*H 6.8; 1.8-fold higher than at pH 7.1.[55] Regardless of the culture temperature, the highest specific growth rate was observed in the range of *p*H from 7.0 to 7.4.[34]

2. 1. 7. Cell Phases of CHO Cell Lines in Bioreactor

When cells are transferred to a new bioreactor batch, they need time to reach stable operation (lag phase). During lag phase cells adapt to new environment and multiply enzymes that are needed to catalyze biochemical reactions.

Initially, concentrations of glucose and other amino acids are falling, while lactate and glutamate (byproducts) concentrations are rising in the medium. After glucose is depleted, lactate starts to get consumed. When substrates are depleted, biomass stops to grow and uses internal reserves to maintain cell functions. Reserve glycogen and lipids are used to supply the cell with the energy. The nutrients from dead cells can be recycled and reused as the energy source. Most commonly used substrate is glucose. If substrate is switched for example to galactose, specific enzymes must be multiplied to reach optimal concentrations, before cells can re-adapt. In the presence of large concentrations of substrates inside cells, mitochondria divide rapidly and supply the cells with large amounts of energy (ATP). Until mitochondria sufficiently multiply, the excess flux of glucose is diverted to lactate or other metabolites, such as alanine.

In the growth phase cells multiply with ease. The lactate does not accumulate anymore and is used up by cells as a substrate. Cells stop to grow when they reach maximum cell density or when they have used up all substrates. Then, cells start to use nutrients from energy storage: glycogen and lipid molecules. When cells run out of the substrates and nutrients from energy storage they enter an atypical cell death due to starvation.

The viable CHO cells are in G1, S, G2/M (part of the interphase) or apoptotic phase.[69,70] The production of protein is usually phase specific.[69,66] In apoptosis cell enter programmed cell death. After certain number of duplications, cells die off. At that time significant amount of biomass in the bioreactor belongs to dead cells.

Table 1: CHO cell metabolic pathways used in reviewed models.

	Alta-mira-no[17]	Jia-ng[46]	No-lan[43]	Quek[5]	Selva-ra-su[45]	San-der-son[50]	del Val[38]	Kram-beck[40]	Jedr-zeje-wski[37]	Zamo-rano[24]	Dean[30]	Yo-ung[15]	Ghor-bani-aghdam[31]	Hag-rot[21]	Nyberg[29]	Sen-gup-ta[2]	Alta mira-no[1]	Xing[3]	Pro-vost[19]	Gou-dar[4]
Glycolysis	YES	YES	YES	YES	YES	YES	no	no	no	YES	YES	YES	YES	YES	YES	YES	YES	YES	YES	YES
Pentose phosphate pathway	YES	YES	no	YES	YES	YES	no	no	no	no	YES	YES	no	no	no	YES	no	no	YES	YES
Lactate production	YES	YES	YES	YES	YES	YES	no	no	no	YES	no	YES	YES	YES	YES	YES	YES	YES	YES	YES
Glycogen synthesis	no	no	no	YES	no	no	no	no	no	no	no	no	no	no	no	no	no	no	no	no
Nucleotide synthesis	no	no	no	YES	no	no	no	no	no	no	no	no	no	no	no	no	no	YES	no	no
TCA cycle	YES	YES	YES	YES	YES	YES	no	no	no	YES	no	YES	YES	YES	YES	YES	YES	YES	YES	YES
Glutaminolysis	YES	YES	YES	YES	YES	YES	no	no	no	no	YES	YES	YES	YES	YES	no	no	YES	YES	YES
Amino acid metabolism	YES	no	YES	YES	YES	YES	no	no	no	YES	no	no	no	YES	no	YES	YES	YES	no	YES
Oxidative phosphorilation	YES	no	YES	YES	no	no	no	no	no	no	no	YES	no	no	no	no	no	no	no	no
Lipid synthesis	no	YES	no	YES	YES	no	no	no	no	no	YES	YES	no	no	no	no	no	no	no	no
Glycosylation	no	no	no	no	no	no	YES	YES	YES	no	no	no	no	no	no	no	no	no	no	no

2. 2. Overview of Important Metabolic Pathways

In the past two decades much research has been done on CHO cell metabolism. At modeling, cell metabolism is described using kinetic laws, equilibrium equations and associated parameters. Table 1 shows metabolic pathways, which were included in the models published in the literature. The following pathways were reviewed: (i) substrate intake, (ii) glycolysis, (iii) glutaminolysis, (iv) pentose phosphate pathway (PPP), (v) UDP-monosaccharides production, (vi) nucleotide synthesis, (vii) amino acid metabolism, (viii) tricarboxylfic acid cycle (TCA), (ix) lipid metabolism, (x) glycogen synthesis, (xi) lipid synthesis, (xii) DNA duplication, (xiii) RNA transcription and protein translation, (xiv) glycosylation, and (xv) feedback loops.

2. 2. 1. Substrate Intake (Part of Metabolic Flux Pathway Analysis)

High influxes of substrates contribute to high osmotic pressure.[71] The cell regulates its pressure with fast conversion into more favorable intermediates and products. Other regulatory mechanisms are passive and active transport. One of the major metabolites is glycogen, which serves as energy storage.[72] Glucogenic amino acids may transform into glucose and then into glycogen, while ketogenic amino acids transforms into ketone bodies that may be stored through acetyl CoA in fatty acids (Figure 2).[73] Mathematical descriptions (Eqs. 18–22) of substrates' consumption are selected in accordance with phenotype, while associated constants are substrate specific. Majority

Figure 2: Biochemical reactions associated with mitochondria: degradation pathway of keto- into glucogenic amino acids.[45] Glucogenic amino acids are transformed into acetylCoenzyme A (AcCoA), while keto amino acids are transformed to glutamate that is further transformed into alpha-ketoglutarate (αKG). Three letter amino acid code is standard. From "A structured, dynamic model for animal cell culture systems," by C. S. Sanderson, J. P. Barford, and G. W. Barton, *Biochem. Eng. J.,* 1999, 3, 203–211. Reprinted with permission.

of the models include glucose intake, lactate, ammonia, CO_2 and oxygen. More precise models include also transport of glutamine and glutamate.

2. 2. 2. Glycolysis and Glutaminolysis (AA Lysis)

Glycolysis is one of the most important pathways in the metabolism of cells and is therefore included in majority of the models (Table 1).[1–5,15,17,19,21,24,29–31,43,45,46,50]

In the growth phase cells extensively use glucose and glutamine. Apart from normal cells, the phenomenon is enhanced in mutated, cancerous cells.[74] Due to osmotic pressure, excess glucose and glutamine are diverted into glycogen,[71] lactate, glutamate, and lipids.[1,16,43,75]

Glucose enters tricarboxylic acid (TCA) cycle through pyruvate (Figure 3). Lactate is a waste product of surplus pyruvate produced during glycolysis that cannot enter TCA cycle due to unavailable mitochondria machinery. Lack of oxygen produces similar effect (Figure 3). Lactate is removed from the cell into the cell medium and later reused.[1,18] Two molecules of ATP and two molecules of NADH are generated in the process. When pyruvate enters mitochondria it is converted into 3 molecules of CO_2. In this process three molecules of NADH, one molecule of $FADH_2$ and one molecule of GTP are produced per molecule of pyruvate. Each molecule of NADH produces three molecules of ATP through electron transport chain; each molecule of $FADH_2$ produces two ATP molecules due to lower proton energy. If lactate is produced, one molecule of NADH is consumed, and recycled when lactate is being converted back. High concentration of lactate may lead to lower *p*H. Note that *p*H is regulated with NH_3 release during glutamate metabolism. Lysis of amino acids gives huge amount of ATP due to independent enzymatic pathways to TCA cycle (Figure 4). In degradation pathways of isoleucine three NADH molecules, one acetyl CoA and one succinyl CoA molecule are generated. ATP is further generated through electron transport chain.

Metabolic models comprise metabolic steps of glycolysis pathway into lumped reactions due to less impor-

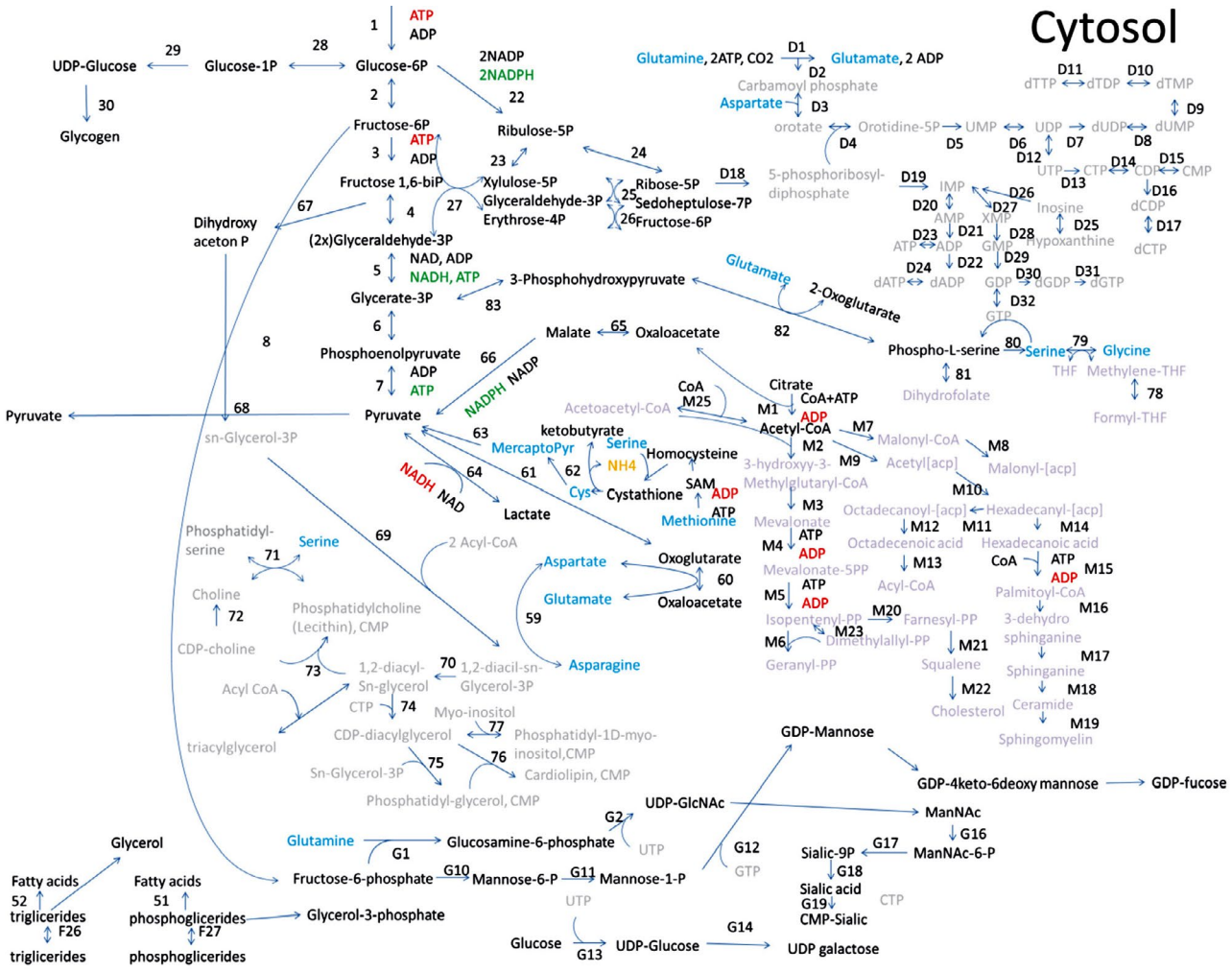

Figure 3: Overview of metabolic pathways in the cytosol: Precise metabolic pathway of catabolism and anabolism in CHO mammalian cell cytosol. Pathways of glucose conversion into pyruvate, glycogen and other monosaccharide's are presented. Formation of nucleotides, lipids, nucleotide monosaccharide's is presented together with cytosolic amino acid synthesis reactions. Amino acids are colored in blue; phosphate rich molecules are colored in green; ADP, NADH in red; gases in orange.[1–5, 13, 15, 17, 19, 21, 29, 30, 45, 46, 50, 76]

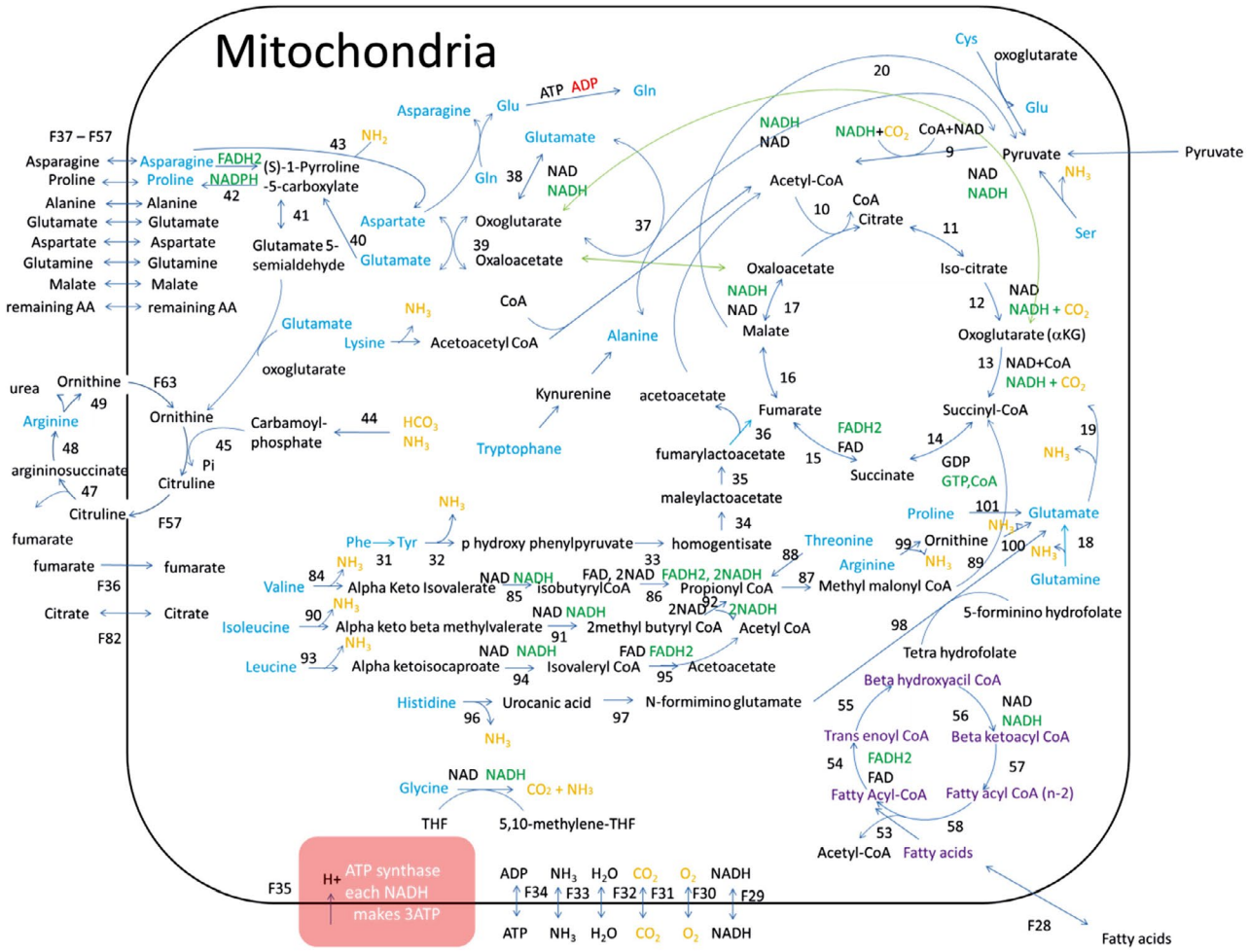

Figure 4: Metabolic pathways within mitochondria: TCA cycle is the major metabolic pathway. Fatty acids are pre-metabolized in beta oxidation cycle (purple). Amino acids (blue) enter TCA cycle through oxoglutarate, fumarate, and succinyl CoA. Oligosaccharides enter TCA cycle through PPP and glycolysis pathway. Gases are colored in orange, while phosphate rich energy molecules are colored in green.[1–5,15,17,19,21,24,29–31,43,45,46,50]

tant, short half-life intermediates.[1–4,17,21,29,46] In simplified models, fluxes are diverted directly to stable intermediates. Complete lysis of amino acids shows that amino acids regenerate intermediates of TCA cycle much faster compared to glycolysis due to independent enzyme machinery of each amino acid. Enormous energy comes from branched chain amino acids (BCAA), i.e. valine, isoleucine, and leucine (Figure 4).

2. 2. 3. Pentose Phosphate Pathway and UDP-Monosaccharides Stock

Like glycolysis, pentose phosphate pathway (PPP) is also included in several models (Table 1).[1,2,4,5,15,17,19,30,45,46,50] An alternative route for glucose is generation of different monosaccharides (Figure 3). From glucose-6-phosphate cell produces ribulose-5-phosphate, xylulose-5-phosphate, erythrose-4-phosphate, fructose-6-phosphate sedoheptulose-7-phosphate and ribose-5-phosphate.[33] Ribose-5-phosphate enters synthesis of nucleotides.[5] Monosaccharides from PPP can be transformed into glyceraldehyde-3-phosphate and fructose-6-phosphate, which again enters glycolysis pathway (Figure 3).

Few models also include generation of UDP-monosaccharides (Figure 3).[37,38,40] In excess of UTP, different nucleotide sugars are generated, including GDP-mannose, UDP-galactose, UDP-glucose, UDP-N-acetyl glucosamine (GlcNAc), and CMP-sialic acid. Nucleotide sugars are included in the models, which describe glycosylation pattern of proteins (Figure 3).[29,37–39] Nucleotide sugars are transported into the endoplasmic reticulum (ER) and the Golgi apparatus (GA), where they get concentrated and ready to be attached to proteins (Figure 3). The attachment is carried out through covalent bond between sugar residue and protein through N-phospho-glycosylation.[37,77]

2. 2. 4. Glycogen Synthesis

Glycogen synthesis is included only in a few models (Table 1),[5] despite its important role in glucose homeosta-

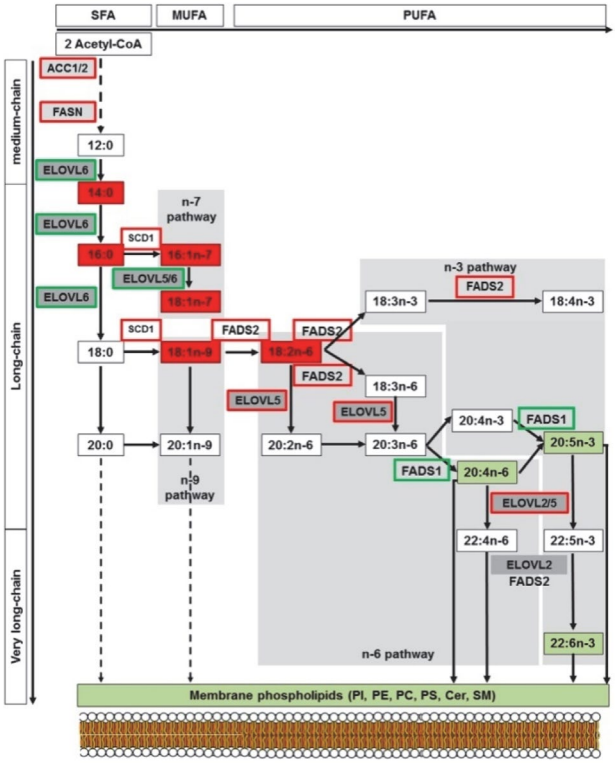

Figure 5: Synthesis of fatty acids from acetyl-CoA: Complex enzymatic pathway leads to different lipid molecules that assemble into membrane bilayer. The saturated fatty acids and unsaturated fatty acids of the n-3, n-6, n-7 and n-9 series can be synthesized from myristic acid (C14) and palmitic acid (C16), produced from ACC and FASN. Long-chain fatty acids of n-6 and n-3 series can also be synthesized from precursors obtained from dietary precursors to elongation (ELOVL) and desaturation (FADS) steps as indicated in the pathways. Lipids marked red and green are "up" and "down" regulated in our analysis, respectively. Increase in enzyme activities is framed in red whereas a decrease is framed in green. ACC: acetyl-CoA carboxylase; ELOVL: elongase of very long chain fatty acid; FASN: fatty acid synthase; FADS: fatty acid desaturase; SCD: stearoyl-CoA desaturase.[78] From "Metabolism dysregulation induces a specific lipid signature of nonalcoholic steatohepatitis in patients," by F. Chiappini, A. Coilly, H. Kadar, P. Gual, A. Tran, C. Desterke, D. Samuel, J. C. Duclos-Vallée, D. Touboul, J. Bertrand-Michel, A. Brunelle, C. Guettier, and F. Le Naour, *Sci. Rep.*, 2017, *7*, 1–17. Reprinted with permission.

sis. In the excess of ATP, cell transfers extra glucose into glycogen that is used as energy source, when glucose is run out from the medium or cytosol. One molecule of glycogen can store up to 30000 molecules of glucose. This contributes to lower osmotic pressure and thus removes harmful effects of high glucose content. Glucose is readily available, if there is a demand on energy or carbon source (Figure 3). The path described above is ATP controlled. Glucose is transformed into glucose-1-phosphate; in this process one molecule of ATP is consumed. UTP molecule binds to glucose-1-phosphate, leading to production of UDP-glucose. UDP-glucose attaches itself to glycogen, leading to release of UDP.

2. 2. 5. Lipid Synthesis

Lipid synthesis is included in several models (Table 1). They used simplified pathways[13,15,17,50,76] or very precisely defined pathways.[5]

During cell division, lipid synthesis is enhanced to simulate assembly of membrane. Phosphoglycerides, triglycerides, phosphatidylserine, phosphatidyllecithine, cholesterol, sphingomyelin, and geranyl pyrophosphate are synthesized (Figure 3). Successive enzymatic pathway starts wih the acetyl-CoA and leads to complex lipid molecules (Figure 5). Different glycerides are synthesized with the addition of fatty acids and other groups to glycerol.

2. 2. 6. Amino Acid Synthesis

Amino acid degradation is described in most models, but usually only partial set of amino acids is integrated in a model (Table 1).[1–5,15,17,19,21,24,29–31,43,45,46,50] Altamirano et al[17] includes synthesis of alanine, aspartate and glutamine in highly interconnected metabolic network. Quek et al[5] describes precise metabolic network with interconnected synthesis of amino acids: alanine, glutamate, asparagine, proline, serine, glycine, aspartate. Provost et al[19] includes synthesis of alanine into the model.

Essential amino acids cannot be synthesized de novo (from scratch) by the organism, therefore must be supplemented from the medium. There are nine amino acids that humans cannot synthesize: phenylalanine, valine, threonine, tryptophan, methionine, leucine, isoleucine, lysine, and histidine (single letter abbreviations in the order they appear: F, V, T, W, M, L, I, K, and H). Other amino acids are synthesized from essential amino acids and other cell intermediates (Figure 6).

2. 2. 7. DNA Duplication, RNA Transcription and Protein Translation

Nucleotides are synthesized through PPP. In a few models nucleotide synthesis is incorporated.[5,19] Provost et al[19] describes highly simplified model. Quek et al[5] describes precise metabolic pathway, where glucose is transformed into ribose, which is further converted to IMP (inosine monophosphate-purine precursor) and UMP (uridine monophosphate-pyrimidine precursor). These precursors are then transformed into ATP, CTP, UTP, GTP, dATP, dCTP, dTTP, and dGTP (Figure 3).

Duplication of DNA and translation of RNAs take place in the cell nucleus. mRNA is transported to the cytosol and rRNA takes position in ribosome, while mRNA is translated into protein by the aid of tRNA. Nucleotide triphosphates (NTPs) are used as an energy source during transcription. For each amino acid, codon is assembled from three NTPs. mRNA is assembled of: 5' cap, 5' and 3' untranslated region (UTR), sequence for signal peptide, coding region, and poly AAA end. mRNA exits the nucleus and enters a ribosome, where the protein is translated

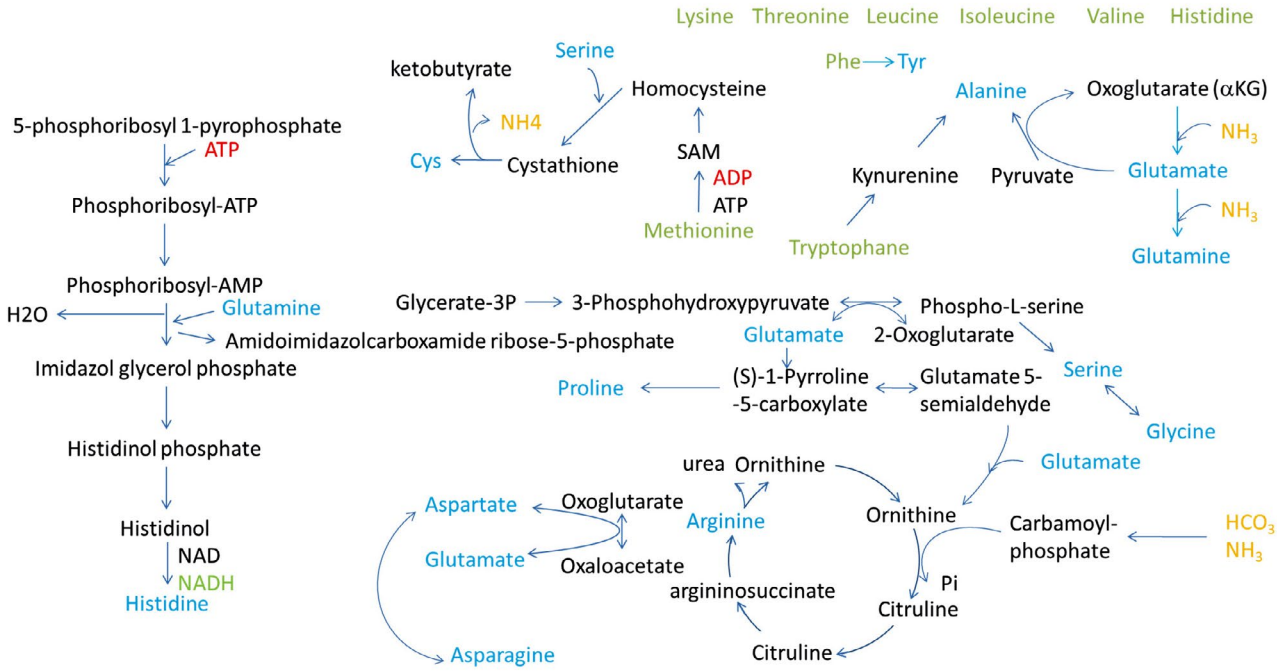

Figure 6: AA synthesis of non-essential amino acids.[1, 5, 19] Synthesis of amino acids from essential amino acids, glycolysis intermediates, carbamoyl phosphate and 5-phosphoribosyl 1-phosphate. Essential amino acids are colored in light green, amino acids in blue, and gases in orange. Energy molecules are colored in green (if produced) or in red (if consummated).

by the help of amino acid-bearing tRNA (AA-tRNA). One ATP molecule is used to create AA-tRNA bond (Figure 7). Transcription and translation are usually not integrated into the models, due to unavailability of data of complex interaction between DNA, amino acids and enzymes.

2. 2. 8. Glycosylation

Glycosylation is the attachment of a glycan unit to a protein after translation. Commonly, it is modeled separately from the rest of the cell metabolism.[37,38,40] Peptide or protein can enter ER, if signal sequence is in front of protein. Inside ER, specific glycans assembled from monosaccharides are attached to the protein through amino residue of the asparagine. Glycan part of the protein is additionally glycosilated in the ER and at the end of this process consists of two N-acetyl glucosamine and nine mannose residues. Afterwards, the glycosylated protein enters the GA where the glycan part of the protein is additionally modified by the help of specific enzymes. N-acetyl glucosamine, galactose, sialic acid, and fucose might be added to final glycan structures. The final products then leave the GA (Figure 7).[77,79] The destination of the glycosylated protein isoforms is determined by a signal peptide in the protein sequence. Glycosylated proteins can be excreted from the cell, incorporated into membrane or transported to other places inside the cell (Figure 7).[77,79]

Availability of glycosylation machinery relative to cellular secretory capacity plays a crucial role in protein glycosylation.[38] A modeling platform is able to predict the distribution of different glycoforms based on extracellular conditions[37] likewise the form of glycan, when expression of the protein is elevated.[40]

2. 2. 9. Feedback Loops

The catabolism is regulated by ATP. High concentration of ATP inhibits conversion of glucose-6-phosphate into ribulose-5-phosphate, fructose-6-phosphate into glycerate-3-phosphate, phosphoglycerate into phosphoenolpyruvate, pyruvate into acetylCoA (glycolysis), glutamine into glutamate, and glutamate into alpha-ketoglutarate (glutaminolysis).[50] ATP also inhibits Krebs cycle in two places: (i) conversion of alpha-ketoglutarate into succinyl CoA, and (ii) oxaloacetate into citrate.[50]

High concentration of ATP slows down catabolism and transfers excess glucose into glycogen. ATP is used for biomass and production of final product. High ATP concentration stops glutaminolysis; glutamine is converted into other amino acids. Glucose is metabolized into nucleotide monosaccharides that are transported into ER and GA. The pathway of glycolysis is highly regulated to sustain sufficient concentration of ATP (Figure 8). In rapidly dividing cells glucose and glutamine consumptions are major steps for energy supply. Both pathways are ATP regulated by negative feedback loop.

High production of lipids from AcCoA and nucleotides from ribose-5-phosphate and glutamine leads to anabolism in CHO cells. DNA is duplicated by the aid of DNA polymerase. Proteins are synthesized in a more com-

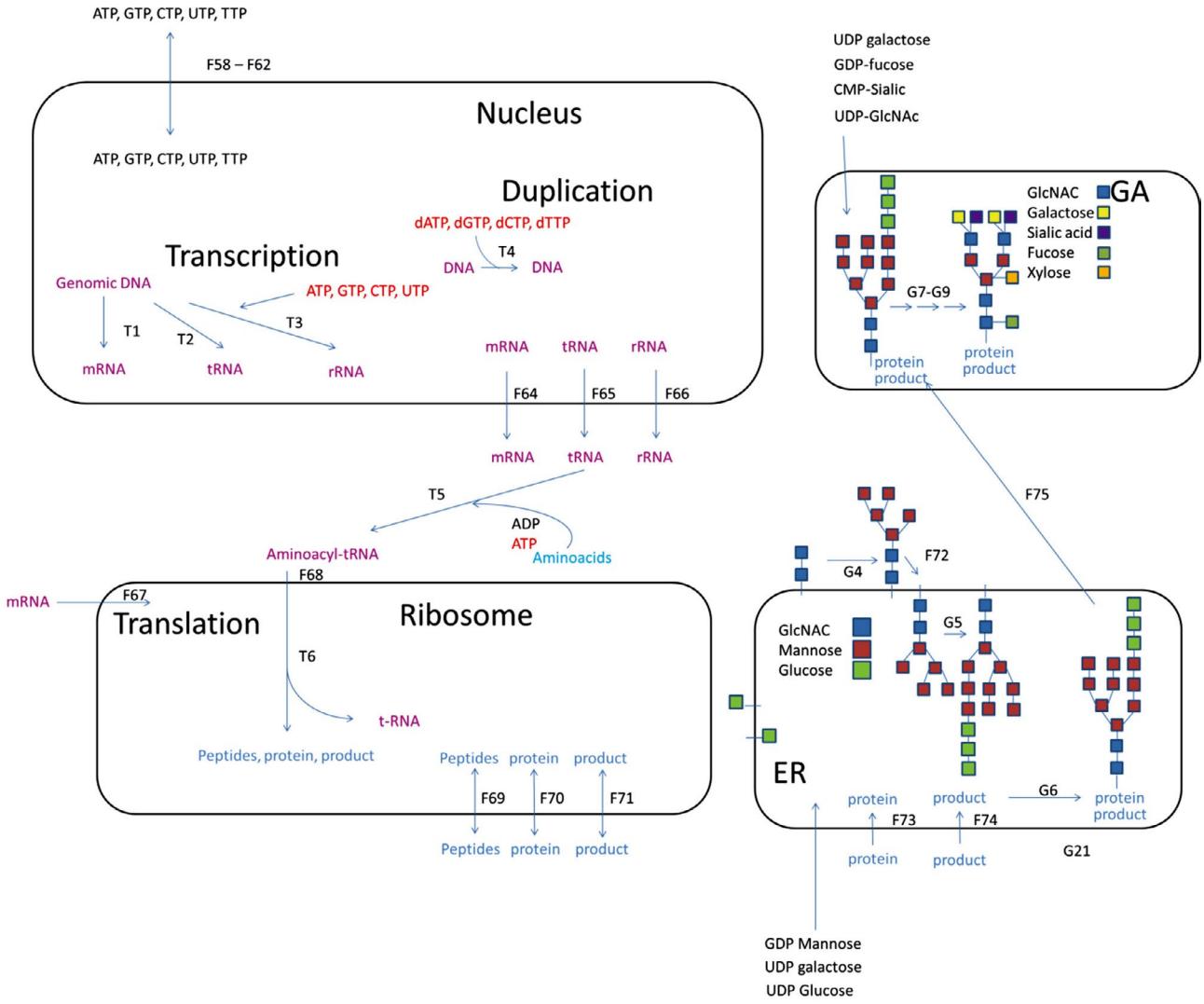

Figure 7: Transcription of DNA takes place in the nucleus, while translation of mRNA takes place in the cytosol. Glycan attachments are done in ER, while associated modifications take place in GA.[5, 19, 37, 38, 40, 77, 79] RNA and DNA are colored in purple, polypeptides are colored in blue. Monosaccharides are labeled with colored square, blue square represents N-acetyl glucosamine unit, red square mannose unit, green fucose, yellow galactose, and orange xylose unit (not added to glycan backbone in CHO cells).

plex way; first transcription of mRNA is needed, followed by translation of proteins by the aid of mRNA, tRNAs, and ribosomes.

2. 3. Mechanistic Models

In addition to black box models, mechanistic models have gained increasing interest in a detailed description of mammalian cell metabolism. Mechanistic models start with a set of metabolites linked up with biochemical reactions, which organize metabolites in the metabolic network. Metabolic network comprises intracellular transformations of metabolites and the membrane transport,

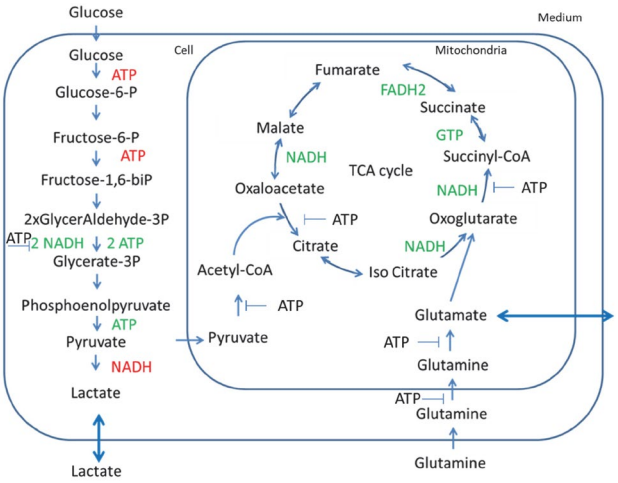

Figure 8: Glycolysis and Glutaminolysis.[5, 50] Molecules colored in green are generated, while molecules in red are used in the transformations. High concentration of ATP stops conversion of pyruvate into acetyl CoA, alpha-ketoglutarate (oxaloacetate) into citrate and oxoglutarate into succinyl CoA.

which couples the cell interior with the cell medium. Metabolic network modeling is commonly associated with the metabolic flux analysis (MFA), flux balance analysis (FBA), and other derived methodologies.[80] MFA considers experimental data to estimate flux rates for biochemical reactions within a metabolic network, while FBA assumes objectives and constraints to tailor the solution space of flux rates. These methods originally provide static insights into metabolic routes, what allows to study cell cultures at a state of particular interest. Even though several extensions were proposed to include extracellular dynamics in the framework of MFA and FBA,[81] precise mathematical representation of reaction kinetics and regulation mechanisms remains a challenge. See the review for a concise overview of metabolic models.[82]

Several attempts have been made to address dynamic behavior of mammalian cell cultures. Nolan et al used the metabolic network with 34 reactions to describe CHO cell metabolism.[43] They used MFA to estimate reactions' flux rates, which were further rationalized by optimization protocols. To imitate the distribution of co-factors they assumed two types: co-factors, which are located within the mitochondria and others within the liquid part of a cytoplasm. They defined the redox variable as the ratio between the rate of generated NADH and the transport rate of NADH from cytosol to mitochondria. The redox variable took place in the kinetic expressions and it was envisaged that governs dynamics of lactate.

Provost et al[19] and later Zamorano et al[24] used MFA and the associated concept of elementary flux modes (EFMs) to recognize probable metabolic routes (macro reactions). They obtain three sets of macro reactions (three submodels), each for the corresponding phase of the cell culture: growth, stationary, and decline phase. Macro reactions were modeled by the Monod kinetic law (Eq. 4). Finally, they assume the interplay between submodels to describe transitions through phases of the cell culture.

In another approach Hagrot et al[21] used the metabolic network with 30 reactions and enumerate the whole EFM spectrum. Then, they used several experimental sets to estimate maximal flux rates of EFMs. Dynamic behavior of EFMs was induced by additional terms that described substrate saturation, product inhibition, and metabolite inhibition. The so-called Poly-pathway model simulated multiple metabolic stages of CHO cell metabolism and thus addresses the diversity seen from experiments. However, the dissemination of the approach toward metabolic networks of larger extent remains a challenge due to time-consuming of EFM enumeration. An example of such models are the genome-scale metabolic models (GEMs), which treat the metabolic network in a more detail together with enzymatic activity and the genome, which encodes enzymes of biochemical reactions in the metabolic network.[45,83] GEMs are phenotype-specific and requires large amount of data and computer facilities. For further reading, see the excellent review of genome-scale approaches.[84]

Mechanistic models have been applied also to study post-translational modifications (glycosylation) of antibodies within mammalian cell cultures.[34,41,85,86] These processes are modeled by three types of kinetic laws, which describe interplay among enzymes and glycoforms: (i) Michaelis-Menten kinetics with competitive and product inhibitions, (ii) Sequential-order Bi-Bi with competitive and product inhibitions and (iii) Random-order Bi-Bi with competitive and product inhibitions. In a greatly accepted approach, authors assume continuous plug flow reactor (PFR) model to represent maturation of glycoforms along the Golgi apparatus.[85] Coupled with the mass balances for nucleotide sugar donors, byproducts, and transport proteins, the PFR model provides a mechanistic explanation for glycosylation profiles of commercial antibodies. Recently, Hutter et al[41] proposed glycosylation flux analysis (GFA) as an MFA analogue to apply constraint-based modeling of the glycosylation network by using a pseudo steady state assumption. Using the GFA, the authors were able to elucidate dynamical changes of glycoforms, caused by media variations.

In our recent work, we proposed a simple metabolic network with 103 biochemical reactions, to investigate transitions between cell phases in mammalian CHO cell cultures.[87,88] Figure 9 shows schematic representation of the metabolic pathways.

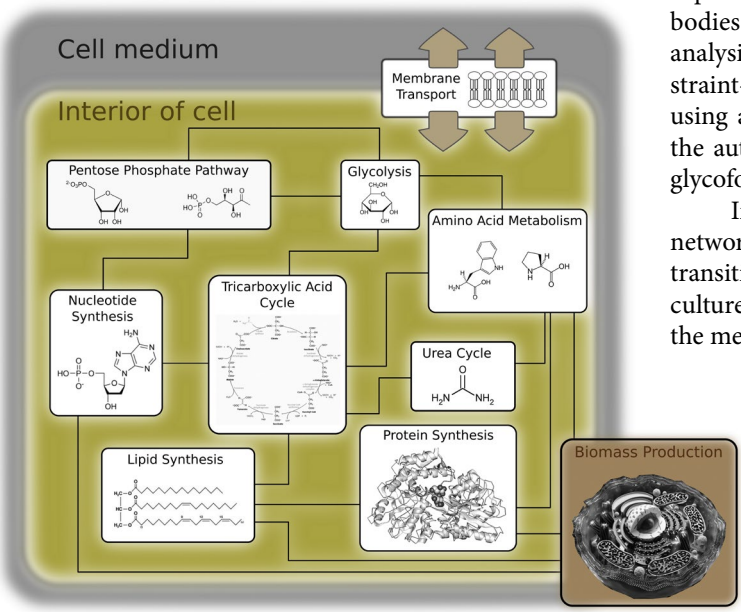

Figure 9: Metabolic network comprises Glycolysis, Pentose Phosphate Pathway, Nucleotide Synthesis, Tricarboxylic Acid cycle, Amino Acid Metabolism, Urea Cycle, Lipid Synthesis, Protein Synthesis Biomass Production, and Membrane Transport. Each pathway comprises detailed set of biochemical reactions, which describes transformations among metabolites on the molecular level.

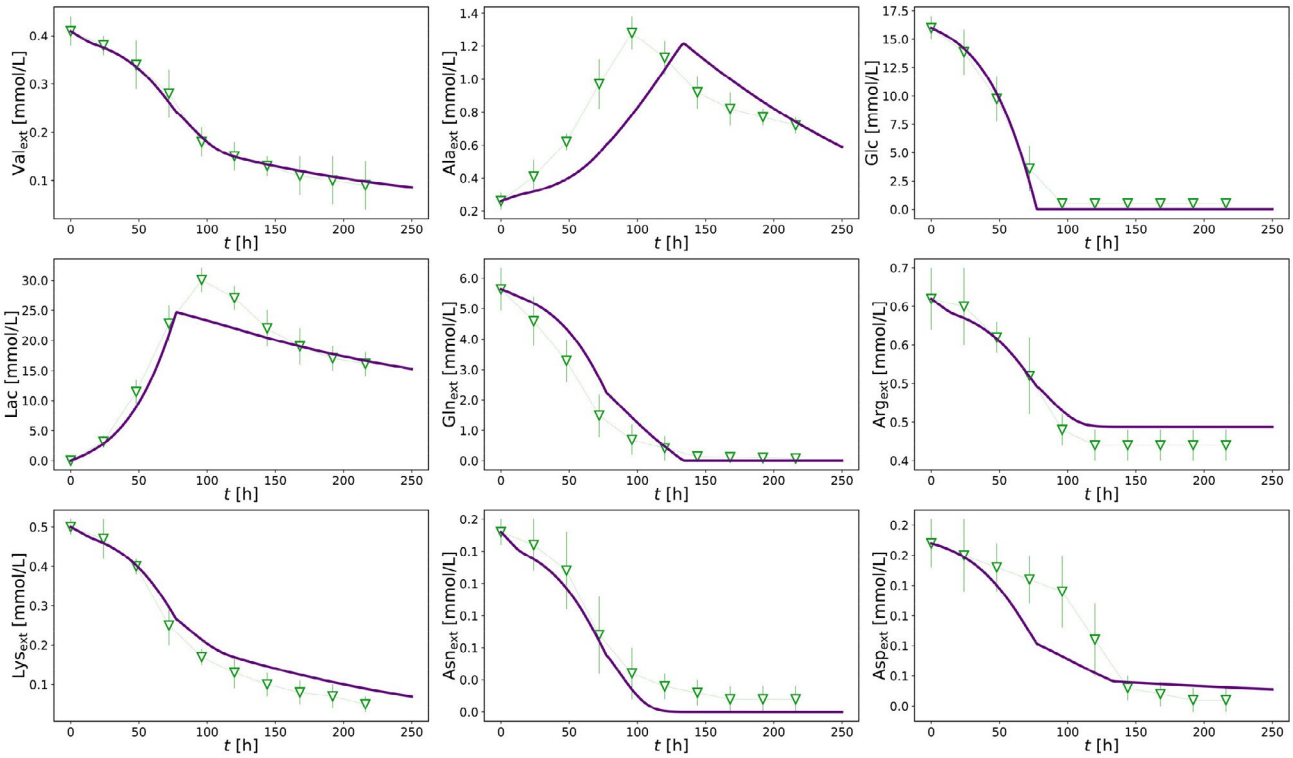

Figure 10: Metabolites' concentration profiles as a function of time. Green points label metabolite uptake or secretion in the cell medium during the cultivation of CHO-320 cells.[13] Purple lines apply to macro reactions, which are characterized by kinetic parameters.[88]

In our approach, the biomass (density of viable cells) evolves as dictated by the cell metabolism, and not via the logistic-typed description (Eq. 1), which is traditionally used in mechanistic models for biomass production. Then, we used the interplay between FBA and MFA to impose constraints within the cell interior, and to estimate the reactions' flux rates. We used the random sampling approach to calculate the set of EFMs (macro reactions), without precalculated EFM spectrum. Assigning Monod kinetic law to macro reactions is a common approach to describe individual phases of the cell culture. Unfortunately, the approach is not suitable to describe transitions between growth, stationary, and decline phase. To overcome this issue, we included negative terms (reversible kinetics) in Monod kinetic law to address inhibition phenomena and the possible rewiring of metabolic routes, caused by products in macro reactions. Description of technical details would be beyond the scope of this review, however we shall mention that after performing the model reduction protocol we achieved evident simplification of the kinetic model. Starting from 64 model parameters we finally obtain 17 kinetic parameters, which turned out to be sufficient to describe dynamics of metabolites in the cell medium. Time evolution of the representative metabolites is shown in Figure 10.

Figure 10 shows characteristics of mammalian CHO cell cultures. At the growth phase, cells exhibit very high consumption rates of Glc and Gln, resulting in high secretion of Lac. Amino acids are mostly depleted. The end of growth phase (t ≈ 90 h) is characterized by Glc deprivation: to compensate it, the produced Lac is consumed as the carbon source instead of Glc as already mentioned.

As seen in Figure 10, the model is capable to describe transitions between cell phases. The important feature of the model turned out to be reversible nature of kinetic expressions, which allow to describe non-monotonic behavior of metabolites' concentrations by means of flux reversal instead of user-defined switching functions that are in general difficult to obtain.

3. Summary

The present review describes how the research should to be done from the start to successfully finish the bioreactor model. In the review we revise recent advances of bioreactor operation and CHO metabolic pathways.

Black box models describe reactor with simple equations that fits curves of growth, substrate consumption and product formation. These are simple formulations that describe working bioreactor with culture at given conditions. Mechanistic models usually describe growth through complex metabolic pathways together with complex operation equations. Black box equations can be also integrated into mechanistic models, a good example is description of biomass growth, where biomass depends on factors inde-

pendent of network metabolic flows. Thorough study of metabolic pathways brings new ideas how to address existing problems that may arise during batch, fed batch and continuous bioreactor operation.

The methodologies we have presented so far are powerful; however there is still an ample room for improvements, which have to be implemented in a consistent way. To improve and extend the current models it is essential to estimate kinetic constants from parallel experiments by measuring response of cell metabolism upon addition of selected nutrients. We expect to gain large benefit by carrying out additional measurements of antibody secretion, which may yield additional flux modes and thus unravel other relevant pathways. Central metabolic pathways should be designed together with glycosylation pathways to form a valuable tool in biotechnology for estimating the quality of product titer. Some of the detailed models we presented have capability to be refined by including the activity of enzymes and their sensitiveness on temperature and pH shifts. Improvements of current methodologies might aid at the development of biotechnology processes and consequentially to facilitate the release of products on the market.

4. Acknowledgements

Special thanks go to partners on the BioPharm.Si project. We are thankful to Dr. Miša Mojca Cajnko for all the help with comments and corrections on the paper.

Funding

This work was supported from program BioPharm. Si co-funded by Republic of Slovenia and European Union from European regional development fund.

Author biographies

Dr. **Jernej Gašperšič** is a researcher with PhD in the field of biomedicine: biochemistry and molecular biology. He has wide interdisciplinary knowledge of biochemistry, molecular biology, chromatography, bioinformatics, computational modeling that was improved in laboratories of institutes and industry. Past work experience is now upgrading with knowledge and expertise in the field of DNA sequencing.

Dr. **Miha Kastelic** received his PhD in 2017 in Chemical Sciences at the University of Ljubljana. Main research activities during his PhD period include protein aggregation, phase equilibrium, statistical mechanics, and associated thermodynamic properties of protein solutions. After his PhD, he joined to the Department of Catalysis and Chemical Reaction Engineering (National Institute of Chemistry) where he utilizes *in silico* methodologies in order to describe central metabolism and glycosylation pathway of mammalian cell cultures.

Dr. **Uroš Novak** has a Ph.D. from Chemical Sciences at the University of Ljubljana. His current focus is in the field of biopharmaceutical up-stream and downstream process engineering and biotechnology.

Assist. Prof. Dr. **Blaž Likozar** earned his PhD in Chemical Engineering in 2008 at the University of Ljubljana, Faculty of Chemistry and Chemical Technology. He has been a member of NIC since 2011, working as a senior research fellow, assistant professor and department head in the field of chemical engineering (Department of Catalysis and Chemical Reaction Engineering); leading the programme "Chemical Reaction Engineering" as well as several research projects. His expertise lies (among others) in heterogeneous catalyst materials, modelling, simulation and optimization of process fluid mechanics, transport phenomena and chemical kinetics. He worked in 2014–2015 at the University of Delaware (Catalysis Center for Energy Innovation, Newark, Delaware, USA), as a Fulbright Program researcher in the field of chemical engineering.

5. References

1. C. Altamirano, A. Illanes, S. Becerra, J. J. Cairo, F. Godia, *J. Biotechnol.* **2006**, *125,* 547–556. **DOI:**10.1016/j.jbiotec.2006.03.023
2. N. Sengupta, S. T. Rose, J. A. Morgan, *Biotechnol. Bioeng.* **2011**, *108,* 82–92. **DOI:**10.1002/bit.22890
3. Z. Xing, B. Kenty, I. Koyrakh, M. Borys, S. H. Pan, Z. J. Li, *Process Biochem*. **2011**, *46,* 1423–1429. **DOI:**10.1016/j.procbio.2011.03.014
4. C. Goudar, R. Biener, K. B. Konstantinov, J. M. Piret, *American Institute of Chemical Engineers Biotechnol.* **2009**, *25,* 986–998.
5. L. E. Quek, S. Dietmair, J. O. Kromer, L. K. Nielsen, *Metab. Eng*. **2010**, *12*, 161–171. **DOI:**10.1016/j.ymben.2009.09.002
6. S. Xu, L. Hoshan, H. Chen, *Bioproc. Biosyst, Eng.* **2016**, *39,* 1689–1702. **DOI:**10.1007/s00449-016-1644-3
7. L. Xie, D. I. Wang, *Biotechnol. Bioeng*. **1994**, *43,* 1175–1189. **DOI:**10.1002/bit.260431123
8. C. A. Sellick, A. S. Croxford, A. R. Maqsood, G. Stephens, H. V. Westerhoff, R. Goodacre, A. J. Dickson, *Biotechnol. Bioeng.* **2011**, *108,* 3025–3031. **DOI:**10.1002/bit.23269
9. M. D. Rocha-Pizana, G. Ascencio-Favela, B. M. Soto-Garcia, M. M. Alvarez, M. D. L. Martinez-Fierro, *Protein Expres. Purif*. **2017**, *132,* 108–115. **DOI:**10.1016/j.pep.2017.01.014
10. H. Hansen, C. Emborg, *Appl. Microbiol. Biotechnol.* **1990**, 41, 560–564. **DOI:**10.1007/BF00178489
11. L. Xie, D. I. Wang, *Biotechnol. Bioeng*. **1996**, *52*, 579–590. **DOI:**10.1002/(SICI)1097-0290(19961205)52:5<579::AID-

BIT5>3.0.CO;2-G
12. H. P. Bonarius, V. Hatzimanikatis, K. P. Meesters, C. D. de Gooijer, G. Schmid, J. Tramper, *Biotechnol. Bioeng.* **1996**, *50,* 299–318. **DOI:**10.1002/(SICI)1097-0290(19960505)50:3<299::AID-BIT9>3.0.CO;2-B
13. F. Zamorano, A. V. Wouwer, G. Bastin, *J. Biotechnol.* **2010**, *150,* 497–508. **DOI:**10.1016/j.jbiotec.2010.09.944
14. C. Goudar, R. Biener, C. Boisart, R. Heidemann, J. Piret, A. de Graff, K. Konstantinov, *Metab. Eng.* **2010,** *12,* 138–149. **DOI:**10.1016/j.ymben.2009.10.007
15. J. D. Young, *Curr. Opin. Biotech.* **2013**, *24,* 1108–1115. **DOI:**10.1016/j.copbio.2013.04.016
16. W. S. Ahn, M. R. Antoniewicz, *Metab. Eng.* **2011**, *13,* 598–609. **DOI:**10.1016/j.ymben.2011.07.002
17. C. Altamirano, A. Illanes, A. Casablancas, X. Gamez, J. J. Cairo, C. Godia, *Biotechnol. Progr.*. **2001**, *17,* 1032–1041. **DOI:**10.1021/bp0100981
18. J. Lopez-Meza, D. Araiz-Hernandez, L. M. Carrillo-Cocom, F. Lopez-Pacheco, M. del Refugio Rocha-Pizan, M. M. Alvarez, *Cytotechnology*. **2016**, *68,* 1287–1300.
19. A. Provost, G. Bastin, *J. Process Control.* **2004**, *14,* 717–728. **DOI:**10.1016/j.jprocont.2003.12.004
20. S. Naderi, M. Meshram, C. Wei, B. McConkey, B. Ingalls, H. Budman, J. Scharer, *Biotechnol. Prog.* **2011**, *27,* 1197–1205. **DOI:**10.1002/btpr.647
21. E. Hagrot, H. A. Oddsdottir, J. G. Hosta, E. W. Jacobsen, V. Chotteau, *J. Biotechnol.* **2016**, *228,* 37–49. **DOI:**10.1016/j.jbiotec.2016.03.015
22. J. Robitaille, J. K. Chen, M. Jolicoeur, *PLoS ONE.* **2015**, *10,* e0136815. **DOI:**10.1371/journal.pone.0136815
23. J. A. Papin, N. D. Stelling,; S. Price Klamt; S. Schuster; B. O. Palsson, *Trends Biotechnol.* **2004**, *22,* 400–405. **DOI:**10.1016/j.tibtech.2004.06.010
24. F. Zamorano, A. V. Wouwer, R. M. Jungers, G. Bastin, *J. Biotechnol.* **2013**, *164,* 409–422. **DOI:**10.1016/j.jbiotec.2012.05.005
25. P. Farzan, B. Mistry, M. G. Ierapetritou, *AIChE J.* **2017**, *63,* 398–408. **DOI:**10.1002/aic.15442
26. B. Berry, J. Moretto, T. Matthews, J. Smelko, K. Wiltberger, *Biotechnol. Progr.* **2015**, 31, 566–577. **DOI:**10.1002/btpr.2035
27. X. Chen, A.P. Alonso, D.K. Allen, J. L. Reed, *Metab. Eng.* **2011**, *13,* 38–48. **DOI:**10.1016/j.ymben.2010.11.004
28. N. E. Lewis, H. Nagarajan, B. O. Palsson, *Nat. Rev. Microbiol.* **2012**, *10,* 291–305. **DOI:**10.1038/nrmicro2737
29. G. B. Nyberg, R. R. Balcarel, B. D. Follstad, G. Stephanopoulos, D. I. C. Wang, *Biotechnol. Bioeng.* **1998**, *62,* 324–335. **DOI:**10.1002/(SICI)1097-0290(19990205)62:3<324::AID-BIT9>3.0.CO;2-C
30. J. Dean, P. Reddy, *Biotechnol. Bioeng.* **2013**, *110,* 1735–1747. **DOI:**10.1002/bit.24826
31. A. Ghorbaniaghdam, O. Henry, M. Jolicoeur, *Bioproc. Biosyst. Eng.* **2013**, *36,* 469–487. **DOI:**10.1007/s00449-012-0804-3
32. B. Ben Yahia, B. Gourevitch, L. Malphettes, E. Heinzle, *Biotechnol. Bioeng.* **2017**, *114,* 785–797. **DOI:**10.1002/bit.26214
33. A. Provost, G. Bastin, S. N. Agathos, Y. J. Schneider, Bioprocess *Biosyst. Eng.* **2006**, *29,* 349–366. **DOI:**10.1007/s00449-006-0083-y
34. S. N. Galleguillos, D. Ruckerbauer, M. P. Gerstl, N. Borth, M. Hanscho, J. Zanghellini, *Comput. Struct. Biotechnol. J.* **2017**, *15,* 212–221. **DOI:**10.1016/j.csbj.2017.01.005
35. Meng Ji, Yelian Miao, Jie Yu Chen, Yebing You, Feilong Liu, and Lin Xu. *Springerplus* **2016,** *5,* 503. **DOI:**10.1186/s40064-016-2151-3
36. Monod J. *Annu. Rev. Microbiol.*, **1949**, *3(1),* 371–394. **DOI:**10.1146/annurev.mi.03.100149.002103
37. P. M. Jedrzejewski, I. J. del Val, A. Constantinou, A. Dell, S. M. Haslam, K. M. Polizzi, C. Kontoravdi, *Int. J. Mol. Sci.* **2014**, *15,* 4492–4522. **DOI:**10.3390/ijms15034492
38. I. J. del Val, K. M. Polizzi, C. Kontoravdi, *Sci. Rep*. **2016**, *6,* 1–16. **DOI:**10.1038/srep28547
39. P. N. Spahn, N. E. Lewis, *Curr. Opin, Biotech*. **2014**, *30,* 218–224. **DOI:**10.1016/j.copbio.2014.08.004
40. J. Krambeck, M. J. Betenbaugh, *Biotechnol. Bioeng*. **2005**, *92,* 711–728. **DOI:**10.1002/bit.20645
41. S. Hutter, T. K. Villiger, D. Bruhlmann, M. Stettler, H. Broly, M. Soos, R. Gunawan, *Metab. Eng.* **2017**, *43,* 9–20. **DOI:**10.1016/j.ymben.2017.07.005
42. E. S. Bayrak, T. Wang, A. Cinar, C. Undey, *IFAC-PapersON-Line*. **2015**, *48,* 1252–1257. **DOI:**10.1016/j.ifacol.2015.09.140
43. R. P. Nolan, K. Lee, *Metab. Eng*. **2011**, *13,* 108–124. **DOI:**10.1016/j.ymben.2010.09.003
44. N. Templeton, K.D. Smith, A. G. Mcatee-Prereira, H. Dorai, M. J. Betenbaugh, S. E. Lang, J. D. Young, *Metab. Eng.* **2016**, *43,* 218–225. **DOI:**10.1016/j.ymben.2017.01.008
45. S. Selvarasu, Y. S. Ho, W. P. K. Chong, N. S. C. Wong, F. N. K. Yusufi, Y. Y. Lee, M. G. S. Yap, D. Y. Lee, *Biotechnol. Bioeng.* **2012**, *109,* 1415–1429. **DOI:**10.1002/bit.24445
46. L. Jiang, A. Boufersaoui, C. Yang, B. Ko, D. Rakheja, G. Guevara, Z. Hu, R. J. Debarardinis, *Metab. Eng.* **2017**, *43,* 198–207. **DOI:**10.1016/j.ymben.2016.11.004
47. J. Berrios, C. Alatmirano, N. Osses, R. Gonzales, *Chem. Eng. Sci*. **2011**, *66,* 2431–2439. **DOI:**10.1016/j.ces.2011.03.011
48. E. E. Gonzo, S. Wuertz, V.B. Rajal, *Biotechnol. Bioeng.* **2014**, *111,* 2252–2264. **DOI:**10.1002/bit.25284
49. Nishikant Shirsat, Avesh Mohd, Jessica Whelan, Niall J. English, Brian Glennon, and Mohamed Al-Rubeai. *Cytotechnology* **2015,** *67(3),* 515–530. **DOI:**10.1007/s10616-014-9712-5
50. C. S. Sanderson, J. P. Barford, G. W. Barton, *Biochem. Eng. J.* ***1999****, 3,* 203–211. **DOI:**10.1016/S1369-703X(99)00021-2
51. T. Goudar, R. Biener, B. K. Konstantinov, J. M. Piret, *Biotechnol. Progr.* **2012**, *25,* 986–998. **DOI:**10.1002/btpr.155
52. P. Jorjani, S. S. Ozturk, *Biotechnol. Bioeng.* **1999**, *64,* 349–356. **DOI:**10.1002/(SICI)1097-0290(19990805)64:3<349::AID-BIT11>3.0.CO;2-V
53. S. R. Chowdhury, J. Djordjevic, B. C. Albensi, P. Fernyhough, *Bioscience Rep*. **2016,** *36,* e00286. **DOI:**10.1042/BSR20150244
54. L. P. Zielinski, A. C. Smith, A. G. Smith, A. J. Robinson, *Mito-*

chondrion. **2016**, *31,* 45–55. **DOI:**10.1016/j.mito.2016.09.003
55. E. Trummer, K. Fauland, S. Seidinger, K. Schriebl, C. Lattenmayer, R. Kunert, K Vorauer-Uhl, R. Weik, N. Borth, H. Katinger, D. Muller, *Biotechnol. Bioeng*. **2006**, *94,* 1033–1044. **DOI:**10.1002/bit.21013
56. W. S. Ahn, M. R. Antoniewicz, *Biotechnol. J*. **2012**, *7,* 61–74. **DOI:**10.1002/biot.201100052
57. Z. Z. Xing, A. M. Lewis, M. C. Borys, Z. J. Li, *Biotechnol. Bioeng.* **2017**, 114, 1184–1194. **DOI:**10.1002/bit.26232
58. N. Jenkins and A. Hovey, *Biotechnol. Bioeng*. **1993**, *42,* 1029–1036. **DOI:**10.1002/bit.260420903
59. B. Rossler, H. Lubben, G. Kretzmer, *Enzyme Microb. Tech.* **1996**, *18,* 423–427. **DOI:**10.1016/0141-0229(95)00121-2
60. S. Becerra, J. Berrios, N. Osses, C. Altamirano, *Biochem. Eng. J.* **2012**, *60,* 1–8. **DOI:**10.1016/j.bej.2011.10.003
61. Watanabe and Okada S., *J. Cell Biol.* **1967**, *32,* 309–323. **DOI:**10.1083/jcb.32.2.309
62. P. Ducommun, P. A. Ruffieux, A. Kadouri, U. von Stockar, I. W. Marison, *Biotechnol. Bioeng*. **2002**, *77,* 838–42. **DOI:**10.1002/bit.10185
63. S. K. Yoon, S. L. Choi, J. Y. Song, G. M. Lee, *Biotechnol. Bioeng.* **2005**, *89,* 345–56. **DOI:**10.1002/bit.20353
64. V. Avello, B. Tapia, M. Vergara, C. Acevedo, J. Berrios, J. G. Reyes, C. Altamirano, *Electron. J.Biotechn*. **2017**, *27,* 55–62. **DOI:**10.1016/j.ejbt.2017.03.008
6.5 N. Kurano, C. Leist, F. Messi, C. Gandor, S. Kurano, A. Fiechter, *J. Biotechnol*. **1990**, *6,* 245–258. **DOI:**10.1016/0168-1656(90)90040-I
66. J. S. Seo, Y. J. Kim, J. M. Cho, E. Baek, G. M. Lee, *Appl. Microbiol. Biot.* **2013**, *97,* 5283–5291. **DOI:**10.1007/s00253-013-4849-2
67. K. Furukawa, K. Ohsuye, *Cytotechnology*, **1998**, *26,* 153–64. **DOI:**10.1023/A:1007934216507
68. H. Kaufmann, X. Mazur, M. Fussenegger, J. E. Bailey, *Biotechnol. Bioeng.*, **1999**, 63, 573–582. **DOI:**10.1002/(SICI)1097-0290(19990605)63:5<573::AID-BIT7>3.0.CO;2-Y
69. R. L. Dutton, J. Scharer, M. Moo-Young, *Cytotechnology*, **2006**, *52,* 55–69. **DOI:**10.1007/s10616-006-9041-4
70. V. Hendrick, P. Winnepenninckx, C. Abdelkafi, O. Vandeputte, M. Cherlet, T. Marique, G. Renemann, A. Loa, G. Kretzmer, J. Werenne, *Cytotechnology* **2001**, *36,* 71–83. **DOI:**10.1023/A:1014088919546
71. M. Rasouli, *Clin. Biochem*. **2016**, *49,* 936–941. **DOI:**10.1016/j.clinbiochem.2016.06.001
72. A. Philip, M. Hargreaves, K. Baar, *Am. J. Phisiol*. **2012**, *302,* 1343–1351.
73. L. Hildebrandt, T. Spennetta, R. Ackerman, C. Elson, E. Shrago, R. T. Ackermann, *Biochem. Bioph. Res. Co.* **1996**, *225,* 207–212. **DOI:**10.1006/bbrc.1996.1171
74. Moncada, S. Higgs, E. A. Colombo, S. L., *Biochem. J*. **2012**, *446,* 1–7. **DOI:**10.1042/BJ20120427
75. O. Feron, *Radiother. Oncol*. **2009**, *92,* 329–333. **DOI:**10.1016/j.radonc.2009.06.025
76. E. J. M. Blondeel, R. Ho, S. Schulze, S. Sokolenko, S. R. Guillemette, I. Sliva, Y. Durocher, J. G. Guillemette, B. J. McConkey, D. Chang, M. G. Aucoin. *J. Biotechnol* **2016**, *234,* 127–138. **DOI:**10.1016/j.jbiotec.2016.07.027
77. E. Maverakis, K. Kim, M. Shimoda, M. E. Gershwin, F. Patel, R. Wilken, S. Raychaudhuri, L. R. Ruhaak, C. B Lebrilla, *J. Autoimmun.* **2015**, *57,* 1–13. **DOI:**10.1016/j.jaut.2014.12.002
78. F. Chiappini, A. Coilly, H. Kadar, P. Gual, A. Tran, C. Desterke, D. Samuel, J. C. Duclos-Vallée, D. Touboul, J. Bertrand-Michel, A. Brunelle, C. Guettier, F. Le Naour, *Sci. Rep*. **2017,** *7,* 1–17. **DOI:**10.1038/srep46658
79. B. Imperiali and S.E. O'Connor, *Curr. Opin. Chem. Biol*. **1999**, 3, 643–649. **DOI:**10.1016/S1367-5931(99)00021-6
80. P. J. D'Huys, I. Lule, D. Vercammen, J. Anné, J. F. Van Impe, K. Bernaerts, *J. Biotechnol*. **2012**, *161,* 1–13. **DOI:**10.1016/j.jbiotec.2012.04.010
81. F. Llaneras, A. Sala, J. Picó, *J. Process Contr*. **2012**, *22,* 1946–1955. **DOI:**10.1016/j.jprocont.2012.09.001
82. E. O. Voit, *WIREs Syst. Biol. Med*. **2017**, 9, e1391.
83. H. Hefzi, K. S. Ang, M. Hanscho, A. Bordbar, D. Ruckerbauer, M. Lakshmanan, C. A. Orellana, D. Baycin-Hizal, Y. Huang, D. Ley, V. S. Martinez, S. Kyriakopoulos, N. E. Jiménez, D.C. Zielinski, L.E. Quek, T. Wulff, J. Arnsdorf, S. Li, J. S. Lee, G. Paglia, N. Loira, P.N. Spahn, L. E. Pedersen, J. M. Gutierrez, Z. A. King, A. M. Lund, H. Nagarajan, A. Thomas, A. M. Abdel-Haleem, J. Zanghellini, H. F. Kildegaard, B. G. Voldborg, Z. P. Gerdtzen, M. J. Betenbaugh, B. O. Palsson, M. R. Andersen, L. K. Nielsen, N. Borth, D. Y. Lee, N. E. Lewis, *Cell Syst.* **2016**, *3,* 434–443. **DOI:**10.1016/j.cels.2016.10.020
84. Ž. Rejc, L. Magdevska, T. Tršelič, T. Osolin, R. Vodopivec, J. Mraz, E. Pavliha, N. Zimic, T. Cvitanović, D. Rozman, M. Moškon, M. Mraz, *Comput. Biol. Med*. **2017**, 88, 150–160.
85. I. J. del VAL, J. M. Nagy, C. A. Kontoravdi, *Biotechnol. Prog.* **2011**, *27,* 1730–1743.
86. T. K. Villiger, E. Scibona, M. Stettler, H. Broly, M. Morbidelli, M. Soos. *Biotechnol Prog.* **2016**, *32,* 1135–1148. **DOI:**10.1002/btpr.2315
87. Kaučič, V. (Ed.), J. Gašperšič, U. Novak, A. Pohar, B. Likozar, *Zbornik referatov in povzetkov, Slovenski kemijski dnevi 2017, Portorož, Slovenia* **2017**, 1–6.
88. M. Kastelic, D. Kopač, U. Novak, B. Likozar, ***2018**, Biochemical Engineering Journal*. https://authors.elsevier.com/tracking/article/details.do?aid=7095&jid=BEJ&surname=Kastelic)

Povzetek

Epitelijske celice kitajskega hrčka (CHO) so ena izmed najbolj uporabljanih terapevtskih medicinskih linij za proizvodnjo različnih biofarmacevtskih zdravil. Imajo visoko stopnjo porabe s hitrim podvajanjem, kar jih naredi idealen biološki klon. Večja količina akumuliranih toksičnih intracelularnih intermediatov lahko privede do nižje viabilnosti organizma, produktivnosti proteinov in proizvedenih bioloških zdravil, zato je potrebna optimalna izbira sestave medija ter bioreaktorskih operativnih parametrov za vodenje bioprocesa. Natančno fenomenološko znanje o biokemijskih transformacijah v celičnem metabolizmu omogoča zaznavo težav, ki se lahko pojavijo med šaržnim, polkontinuirnim in kontinuirnim obratovanjem bioreaktorja. Za boljše razumevanje (in povezave), so bili izdelani mehanistični modeli, ki se lahko uporabijo za optimiziranje obratovanja in povečevanja skale. V tem delu je narejen pregled glavnih metabolni poti v strukturiranih sesalskih kulturah CHO. Pregled se začne z biokemijskim ozadjem znotraj celica, ki nadzirajo povezane pojave in kinetiko, ki urejajo vzpostavljene biološke poti. Nato sledi opis posamezne pretvorbene poti, preko pregleda standardnih matematičnih formulacij, ki se običajno uporabljajo v inženirstvu. Te formulacije sledijo principu modeliranja t.i. črne škatle (black box), ki povezuje substrate/produkte na poenostavljen način. Poleg tega so predstavljeni modeli, ki vključujejo analizo metabolnih fluksov (MFA) in analizo uteženih fluksov (FBA). Na koncu je pregled podobnosti med različnimi pristopi za njihovo strukturno zasnovo. Izpostavljene so enačbe s spremenljivkami, ki se uporabljajo za opis rasti kontroliranih pogojev v bioreaktorju, raziskane reakcijske serije rasti populacije CHO, povezane z vrednostmi maksimalne encimske aktivnosti. Procesi so našteti tako, da lahko bralec integrira najsodobnejši pristop. Posebej je izpostavljen tudi prispevek avtorjev.